Academic Science Journal

Effect of Zinc and copper co-doping for Cadmium Oxide Thin Films on NO_2 and H_2S Gases Sensitivity

Roaa J. Mohammed* **and J. Alzanganawee**

Department of Physics, College of Science, University of Diyala, Diyala, Iraq

*sciphydr2108@uodiyala.edu.iq

Received: 3 June 2024 **Accepted: 18 August 2024**

Published: October 2025

DOI: https://dx.doi.org/10.24237/ASJ.03.04.890B

Abstract

In this work, the Sol-gel spin coating process is used to synthesize pure and co-doping (Zn:Cu)% CdO thin films on glass substrates for using it as gas sensors for NO_2 and H_2S. A range of characterization techniques are utilized to assess the structural, optical, electrical, and sensing properties of the prepared thin films. These techniques include X-ray diffraction (XRD), atomic force microscopy (AFM), field emission scanning electron microscopy (FE-SEM), energy-dispersive X-ray spectroscopy (EDS), UV-vis measurements, Hall Effect measurements, and sensitivity measurements. All films have a cubic crystal structure and are polycrystalline, according to XRD measurements. The co-doping ratio rose from 0% to 3%, resulting in an increase in the optical band gap values from 2.53 to 2.58 eV. AFM scans show that with co-doping, roughness and particle size gradually decrease. The form and size of the grains altered with the co-doping, according to FE-SEM analysis. EDS analysis additionally verified that O, Cd, Zn, and Cu present in the original solution. All films have n-type charge carriers, according to Hall Effect tests, doping caused increase carrier concentrations and better conductivity. At different temperatures, the sensitivity, responsiveness, and recovery time of the gas sensor

assessed. At 200 °C, pure and (3%Zn:3%Cu) co-doped CdO thin films showed optimal sensitivity of 45.9% and 129%, respectively, for the NO_2 and H_2S sensors.

Keywords: CdO, co-doping, AFM, FE-SEM, EDS, gas sensitivity, NO_2, H_2S.

Introduction

Because of the ongoing progress of industrialization, the concentration of poisonous and hazardous gases, such as NO_2, H_2S, CO_2, SO_2, and volatile organic compounds (VOC), is increasing fast in the environment [1]. One of the primary harmful substances released from automobile exhaust is NO_2, which is also a primary component of emissions from indoor appliances. Moreover, it changes the atmosphere to produce hazardous organic nitrates and gaseous nitric acid, which helps to create acid rain. As a result, for ongoing monitoring of emission processes, a precise and selective NO_2 sensor is crucial [2]. Regarding hydrogen sulfide (H_2S), is a very toxic and combustible gas known as manure gas and sewage gas [3]. It frequently gathers in closed spaces with poor ventilation, like sewage lines, basements, and Manholes. It often starts with organic debris broken down by bacteria in anaerobic conditions. It can also happen in geothermal systems, where heat metamorphism and magma degassing are sources. In addition, H_2S is generated as a byproduct in over 70 sectors, such as waste management, coal gasifiers, Kraft paper mills, petroleum refining, and natural gas extraction [4]. Consequently, H_2S detection is crucial.

By interacting with the metal oxide film's surface, the target gas alters the material's charge carrier concentration, usually by surface-adsorbed oxygen ions. The material's conductivity (or resistivity) is changed as a result of this shift in charge carrier concentration [5].

Many studies during the last few years have shown that “metal-oxide-semiconductors” can be vastly employed as detectors to distinguish between different gases [6]. To reveal a tiny amount in a drastic environment, metal-oxide-depending detectors' sensing capabilities must be improved for superior selectivity and quick response/recovery times. According to numerous studies, adding the right substance into a semiconductor lattice can increase the sensitivity as well as selectivity of semiconducting metal-oxide-based sensors [7-9].

Researchers gave a lot of attention on cadmium oxide (CdO), an n-type semiconductor, in the process of creating solar cells and optoelectronic devices. CdO hasn't, however, been thoroughly investigated as a gas-detecting material yet. It is necessary to do further research on the function of nanocrystalline CdO as a gas sensor among the various metal-oxide gas sensing materials [10].

In this study, glass substrates were coated with pure CdO and (Zn:Cu)% co-doped CdO thin films using the sol-gel spin coating process. The goal of this work is to evaluate the impact of co-doping on the structural, surface, optical, electrical, and gas-sensing characteristics of CdO thin films.

Material and Methods

Precursor materials include cadmium acetate dihydrate, 2-methoxyethanol, zinc acetate dihydrat, copper acetate dihydrat, and monoethanolamine (MEA). First, the CdO precursor solution made by using the sol-gel spin coating method. 0.5 M of cadmium acetate dihydrate, or $Cd(CH_3COO)_2 \cdot 2H_2O$, was dissolved in 1:10 2-methoxyethanol ($C_3H_8O_2$) and continuously agitated for 20 minutes at 27 °C. After that, a homogenous, clear solution was achieved gradually by adding mono-ethanolamine (C_2H_7NO; Abridged MEA) as a stabilizer. This was done while stirring continuously and heating the mixture at 75 °C for two hours. After that, the mixture was left to age for a day at room temperature until the gel took shape. Using a spin coater, the clean substrate was covered with the viscous homogeneous solution to create a thin layer (L2001A3-E461-UK). All of the films were processed using the same set of parameters: 3300 rpm for rotation and 35 s for time. After drying the films for 20 minutes at 200 ◦C, the process was repeated five times, resulting in five coatings of the sample that were subsequently annealed for one hour at 475 ◦C. Similar to this setup, co-doped CdO thin films were produced by adding zinc acetate ($Zn(CH_3COO)_2.2H_2O$) and copper acetate ($Cu(CH_3COO)_2.2H_2O$) to a solution and heating it continuously with magnetic stirring. The ratio of Zn to Cu were (1:1)% and (3:3)%, respectively.

By analyzing XRD patterns using Cu-Kα radiation (λ= 1.54056 Å) and an X'pert PANalytical system in the 2θ range of 20◦ to 80◦, the crystalline nature of the produced films was examined. Using an FE-SEM (ZEISS-EVO 18), the surface morphology of the produced films was examined. Optical research was conducted using a Perkin Elmer spectrometer (Model: Lambda-35) for AFM. Using van der Waals geometry and the four-probe approach, the Hall Effect was measured. The results were discussed.

Results

X-ray diffraction studies

Figure (1) displays the XRD patterns of pure CdO, 1:1, and 3:3 (Zn:Cu) thin films. Without any impurities or secondary phases, the produced films' XRD pattern showed peaks at (111), (200), (220), (222), and (311) directions. Additionally, there is good agreement between the obtained diffraction peaks in the XRD patterns and the standard data for CdO (ICDD 75-0592).

According to the XRD examination, all of the produced CdO thin films have a preferred orientation along the (111) plane and are polycrystalline. The findings are in good agreement with [11] and demonstrate that the films' crystallinity reduces with doping and increases with increases in the concentration of (Zn:Cu) co-doping. Pure CdO and Zn:Cu co-doping CdO have slightly lower lattice parameter values (4.9648) than those found in ICDD (75-0592). Pure CdO film has a high lattice parameter. On the other hand, Zn:Cu co-doping in CdO lowers the lattice parameter. The reason for the decrease in the lattice parameter when Zn and Cu ions are co-doped is because their ionic diameters are smaller than those of Cd^{2+} [12].

The different full width at half maximum (FWHM) (β) values indicate that doping has an impact on the crystallite size of CdO films. Using standard relations, a few other parameters were determined, including texture coefficients (TC), microstrain (ε), number of crystallites per unit area (N), and dislocation density (δ). The formula for Debye Scherrer was used to calculate the crystallite size (D) of CdO films. It may be found in the equation [12]:

$$D = \frac{K\,\lambda}{\beta_{2\theta}\,\cos\theta} \quad (1)$$

where $\beta_{2\theta}$ is the diffraction peak broadening measured at half of its maximum intensity (degrees), or FWHM, and K is the shape factor, which is equal to 0.94.

The dislocation density and microstrain of the films were also calculated using the crystallite size measurements and the following relations [13]:

$$\delta = \frac{1}{D^2} \quad (2)$$

$$\varepsilon = \frac{\beta\cos\theta}{4} \quad (3)$$

For the (Zn:Cu) co-doped CdO films, the crystallite size (D) ranges from 35.60 to 30.95 nm on average. The following formula [14] was used to determine the dislocation density and number of crystallites (N) per unit volume for various CdO thin film doping concentrations:

$$N = \frac{1}{D^3} \quad (4)$$

It is found that the pure CdO thin films have lower dislocation density and fewer crystallites per unit surface area. Because of the high (111) peak intensity, this result indicates that the CdO thin film has a comparatively greater crystalline quality when it is compared to other samples. The following equation [15] was used to calculate the optimal orientation using the TC:

$$TC(hkl) = \frac{I(hkl)/I_{\circ}(hkl)}{N_r^{-1}\sum I(hkl)/I_{\circ}(hkl)} \quad (5)$$

where (N) is the number of peaks in the experimental pattern, Io(hkl) is the intensity that was noticed, and I (hkl) is retrieved from the ICDD data. The fact that (Tc) values exceed one indicates that there are more grains in a particular (hkl) direction.

Table (1) displays the computed values for the microstructural characteristics of the CdO thin films in the (111) plane, including D, δ, ε, N, and TC.

Academic Science Journal

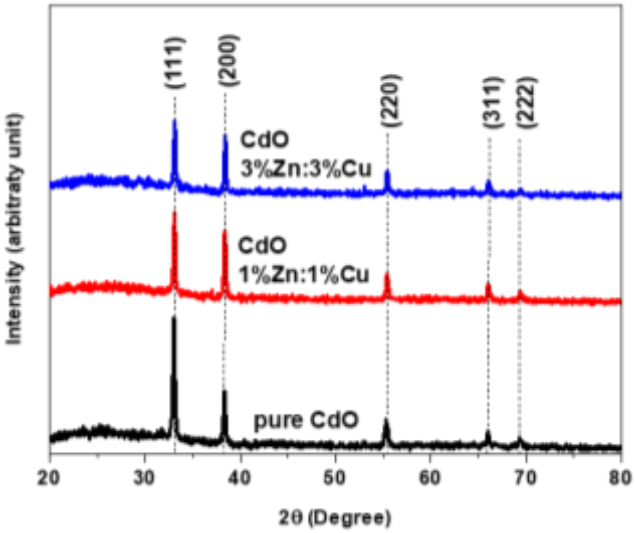

Figure 1: XRD patterns of CdO and Zn:Cu co-doped thin films

Table 1: The structural parameters of pure CdO and Zn:Cu co-doping CdO thin film.

Sample	2θ°	FWHM	$D_{(111)}$ (nm)	a (111) Å	$\delta\times10^{-3}$	$\varepsilon\times10^{-3}$	$N\times10^{-3}$	Tc (111)
Pure CdO	33.03	0.24	35.60	4.6934	0.789	1.017	8.643	1.5
CdO (1%Zn:1%Cu)	33.13	0.31	27.90	4.6791	1.285	1.297	17.965	1.1
CdO (3%Zn:3%Cu)	33.11	0.28	30.95	4.6826	1.044	1.170	13.158	1.09

Surface studies

AFM analysis

Using AFM analysis, the topography of prepared thin film surfaces was investigated (Figure 2). Dense, irregular grains that are uniformly dispersed across the film's surface are visible in a pure film. Furthermore, when the dopant concentration is 1% Zn:1% Cu, spherical, unevenly dispersed grains are observed to develop. This phenomenon may be the result of nucleation brought on by the substitution of Zn and Cu. We see that the granule density increases, organization and distribution become more homogeneous as the doping concentration rises.

After doping it was observed the particle size and average film roughness decreased. This is due to the difference in the ionic radii of copper and zinc with cadmium, which in turn leads to the improvement of nucleation and the enhancement of the surface diffusion of the impurity atoms as a result of the increased its mobility, which allows to rearrange easily and remove surface

defects. This result is consistent with the XRD measurements. Table 2 includes tabular data on topographic parameters, including particle size, average roughness (Ra), and root mean square roughness (Rrms).

Table 2: Average roughness, root mean square and particle size value of the sample.

Sample	Average roughness (nm)	RMS roughness (nm)	Particle size (nm)
Pure CdO	75.90	86.78	212
CdO (1%Zn:1%Cu)	30.79	37.05	148
CdO (3%Zn:3%Cu)	37.72	45.04	208

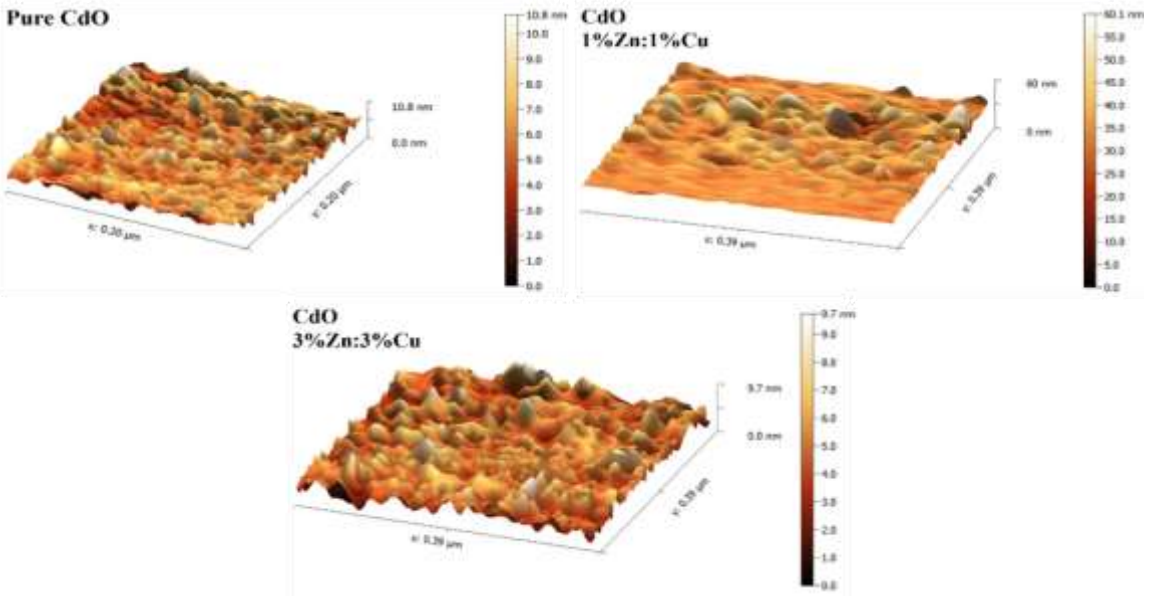

Figure 2: AFM topo graphs of pure and (Zn:Cu) co-doped CdO thin films

FE-SEM analysis

Figure (3) shows a comparison of the surface morphology of CdO thin films as a function of Zn:Cu doping concentration using FE-SEM analysis. The equally dispersed grains resembling cauliflower and some voids make up the pure CdO thin film. Report [16] likewise reports the same FE-SEM picture. The doped thin film samples by 1:1 and 3:3 (Zn:Cu) exhibit surface morphology characterized by comparatively large sphere-like grains with small voids. With an increase in doping concentration from 0 to 1%Zn:1%Cu and a subsequent decrease to 84 nm for 3%Zn:3%Cu, the average grain size went from 56 to 87 nm.

Improved crystalline quality and a decrease in the overall grain border percentage in the films are caused by the increased average grain size, which can also lessen grain boundary scattering and, as a result, lower electrical resistivity [17]. The discussion above makes it abundantly evident that, as compared to pure and 1%Zn:1%Cu co-doped CdO thin films, the co-doping by zinc and copper efficiently modified the surface of CdO thin films, especially by (3:3) has uniformly dispersed grains.

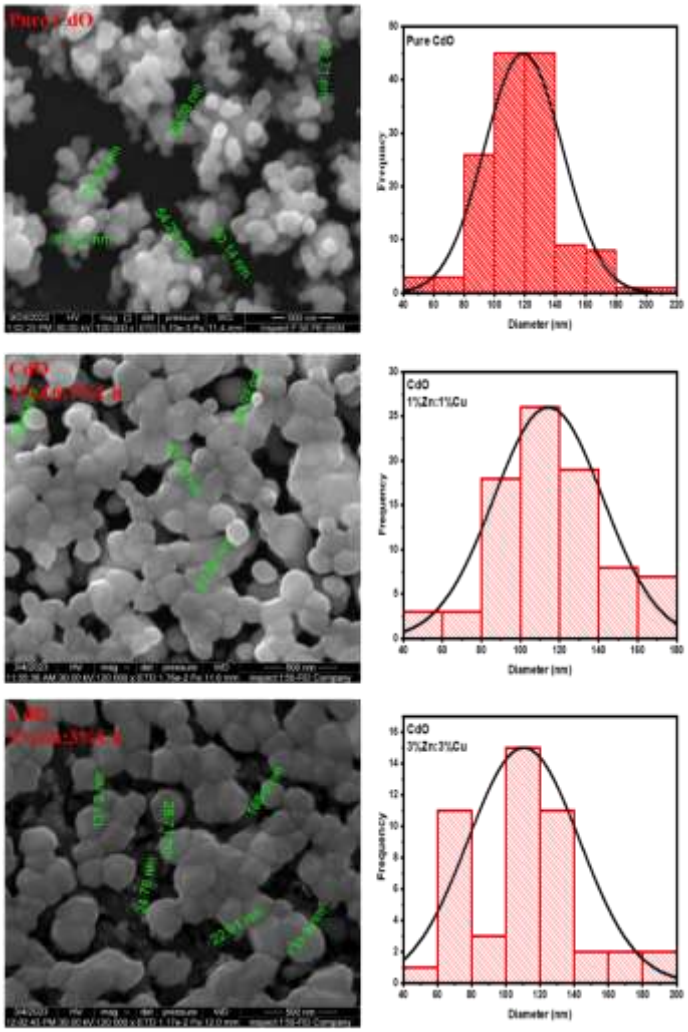

Figure 3: The FE-SEM micrographs and histogram of pure CdO, 1% and 3% (Zn:Cu) co-doped CdO thin films.

Academic Science Journal

Figure (4) displays the "cross-sectional FE-SEM images" of prepared films. As evidenced by the material's diffusion into the substrate, the thickness of the coated films was found to be consistent throughout the layer, indicating strong adhesiveness to the surface. For the remaining samples, the variation in the (Zn:Co) co-doped contents has altered the side form and thickness of the coated films. The thickness that was observed exhibited a reduction with doping.

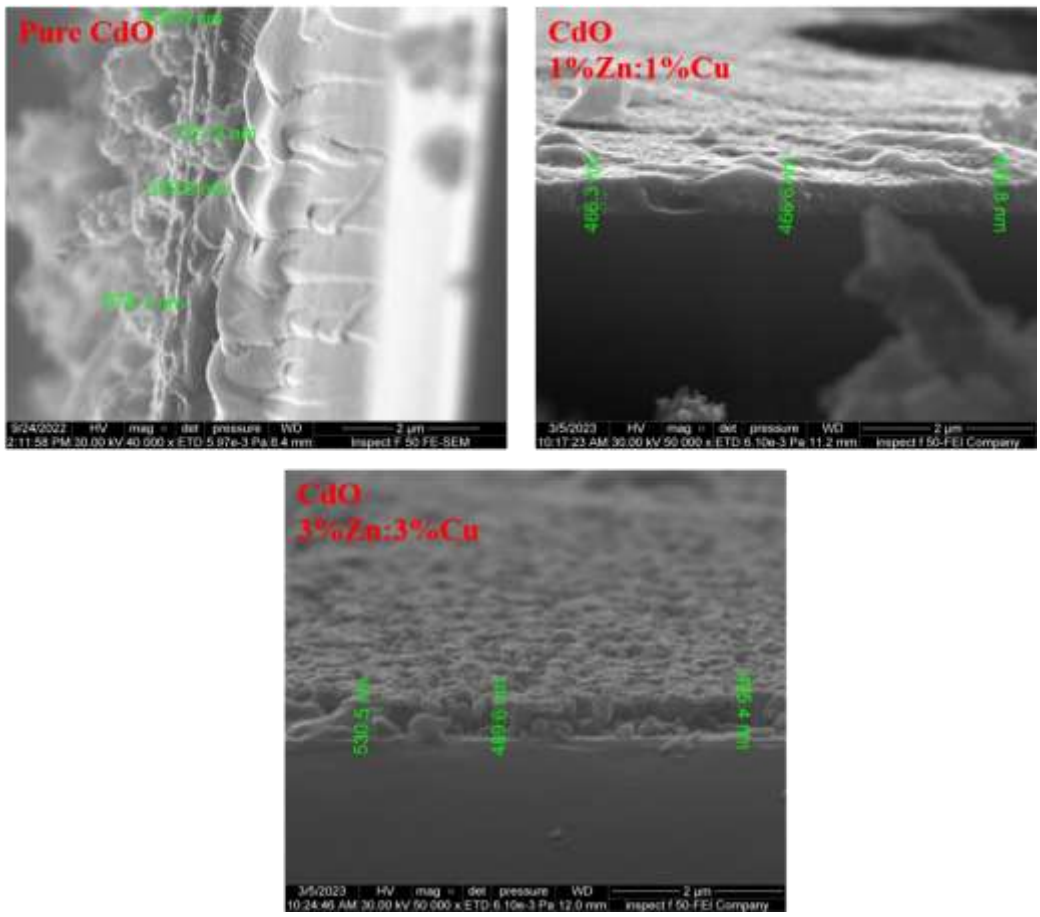

Figure 4: The cross-sectional FE-SEM images of pure CdO, 1% and 3% (Zn:Cu) co-doped CdO thin films

Elemental analysis

The elemental analysis is performed using energy-dispersive spectroscopy (EDS) on pure and (Zn:Cu) co-doped CdO thin films. Figure (5) displays the EDS spectra of both pure and (Zn:Cu) co-doped CdO thin films, confirming the presence of Zn and Cu in the films.

Academic Science Journal

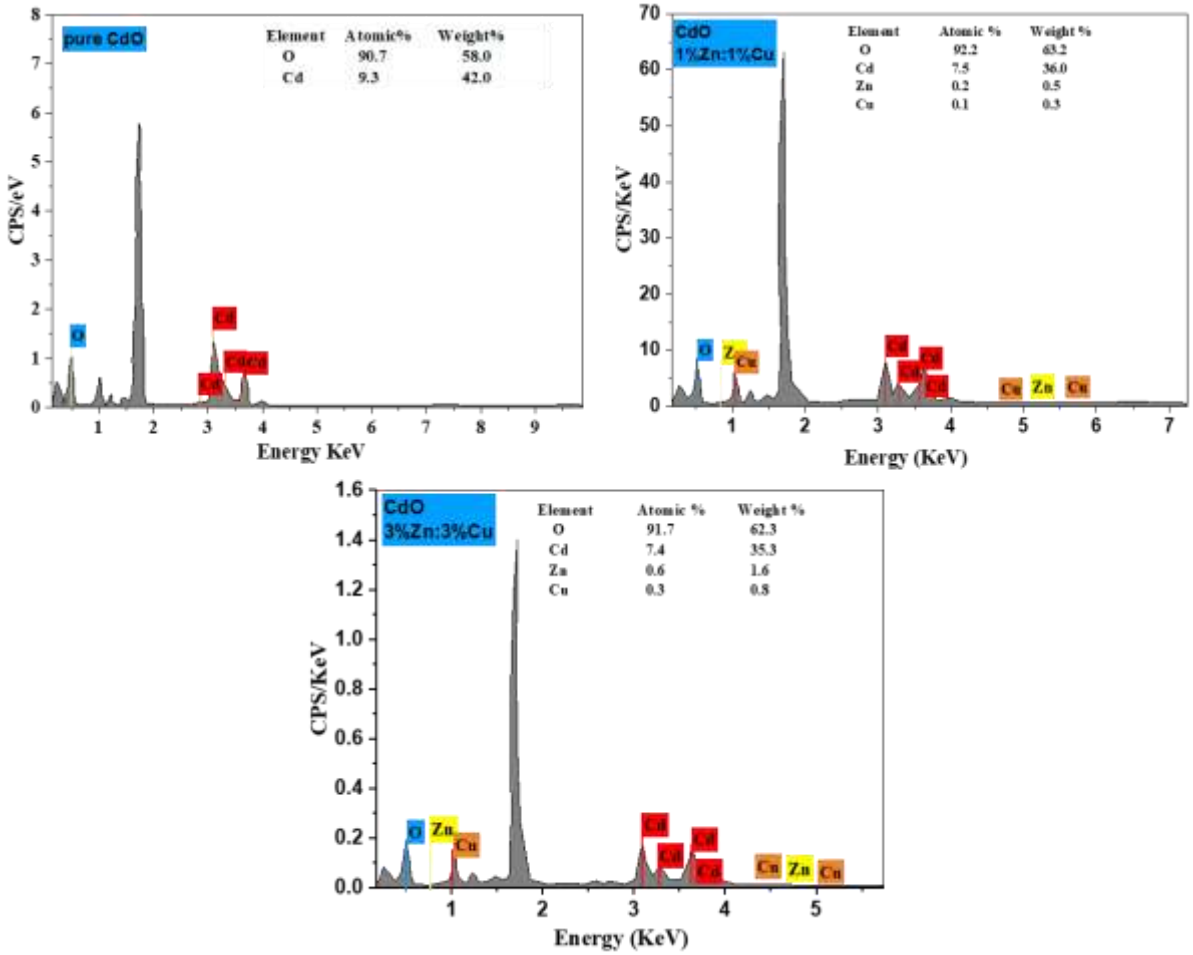

Figure 5: EDS spectrum of pure CdO, 1% and 3% (Zn:Cu) co-doped CdO thin films

Optical studies

The following formula was used [11] to determine the optical bandgap of pristine and Zn:Cu doubly doped CdO thin films:

$$\alpha h\nu = A\,(h\nu - E_g)^2 \qquad (6)$$

where Eg is the optical bandgap energy, hv denotes incident photon energy, and α represents the absorption coefficient. As it is shown in Figure (6), the straight portion of the curve can be projected to the x-axis (hv axis) to determine the Eg.

From the Figure (6) we noticed that the energy gap increases with doping and this is due to quantum confinement effects brought on by the reduction in crystallite size as a result of the doping of zinc and copper [18]. The literature [19–23] also noted these increases in optical

bandgap energy values caused by Zn or Cu doping concentrations. Figure 7 shows the spectrum of transmittance of prepared films. It is clear from Fig. 7 that double doping improves transmittance. For pure and Zn:Cu double-doped CdO films, the recorded transmittance values are approximately 85% and 97%, respectively. As previously it was noticed [24], reduced scattering effects, greater crystallinity, and structural homogeneity could all contribute to increased transparency. The doped films' transparency may have grown as a result of improved surface smoothness brought on by reduced crystallite size [25].

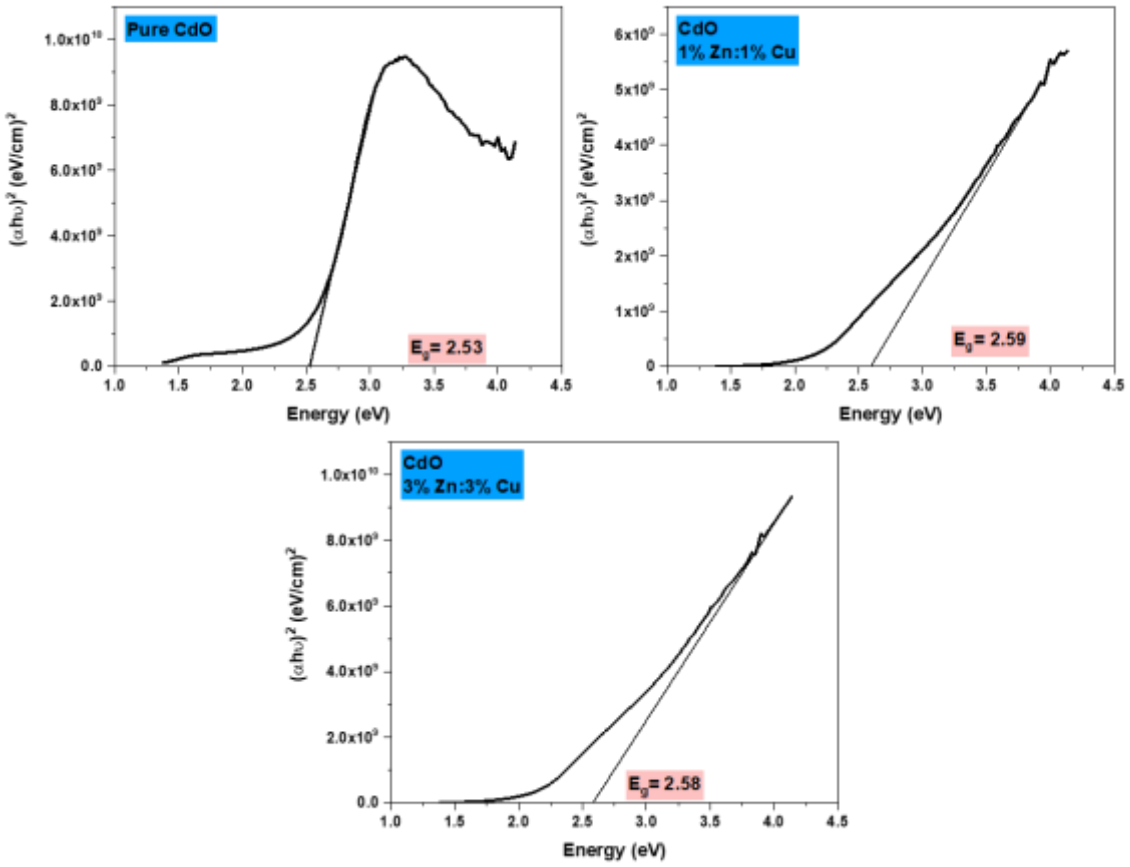

Figure 6: $(\alpha h\nu)^2$ vs. photon energy plots of pure CdO and (Zn:Cu) co-doped CdO thin films.

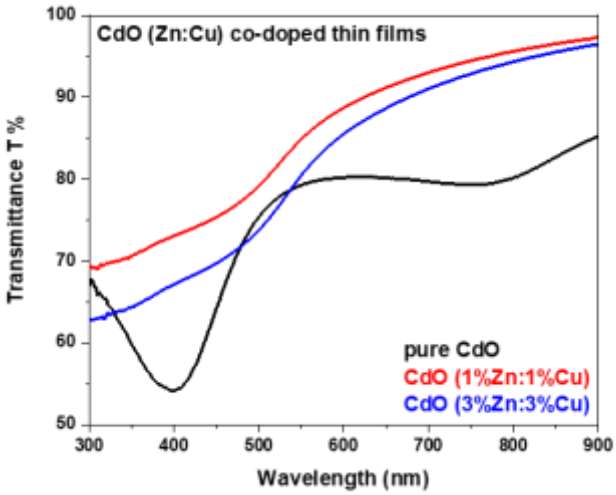

Figure 7: The spectrum of transmittance of pure CdO and (Zn:Cu) co-doped CdO thin films

Electrical studies

The kind of majority carriers of charge, their density, and their mobility are all displayed by studying the Hall Effect of thin films, which provides a clear representation of the nature of semiconductor conduction. Every prepared film was n-type, according to the Hall Effect measurement. From the Table (4) we can notice that conductivity increased with doping. The increase in conductivity is attributed to the increase in carrier concentration resulting from substitutional defects in the lattice [26]. The decrease in mobility of charge carriers may be due to increase in grains boundaries owing to decrease in crystallite size with doping.

Table 4: The variation of the electrical parameters of the pure, 1% and 3% (Zn:Cu) co-doped CdO films.

Sample	Carrier concentration (n) (cm^{-3})	Mobility (μH) (cm^2 /Vs)	Conductivity σ(Ω^{-1} cm^{-1})	Type
Pure CdO	-2.11×10^{18}	223	0.75	n-type
CdO (1%Zn:1%Cu)	-29.00×10^{18}	35	1.62	n-type
CdO (3%Zn:3%Cu)	-19.00×10^{18}	76	2.31	n-type

Gas sensor studies

By using an on-and-off gas switch, the prepared films were exposed to NO_2 and H_2S gases to examine the variations in resistance over time. The samples in question were spin-coated glass

substrates containing pure CdO, 1%Zn:1%Cu, and 3%Zn:3%Cu co-doping CdO thin films. The operational temperatures in the experiment ranged from 100 to 300 °C. It is worth noting that measuring the sensitivity at room temperature was tried, but no sensitivity value was obtained, and the sensitivity measurement were not successful at temperature less than 100 °C. The active surface of the sensor absorbs oxygen molecules from the ambient air. Subsequently, these molecules undergo ionization through the removal of electrons from the sample surface's conduction band. A surface depletion layer and several oxygen ion types are produced as a result of this process [28].

The amount of gases that have been adsorbed determines the depth of the depletion layer, which may form barriers that prevent charge carriers from passing through the channels between neighboring nanoparticles. Oxidizing gases tend to take electrons from sample surfaces when they come into contact with them, which lowers charge carrier mobility and concentration. The deepness of the layers of surface depletion changes as a result of this interaction. When the sample is exposed to oxidizing gasses, its resistance increases [29]. The resistance change as a function of time with an on/off gas valve for NO_2 and H_2S gases with concentrations of 125 (PPM) and 50 (PPM), respectively, is displayed in Figures (8, 9, and 10). As the gas switch is open, the resistance rises. Because NO_2 is an oxidizing gas, the resistance quickly drops as the gas is turned off. On the other hand, when using reduced H_2S gas, the resistance behavior is opposite.

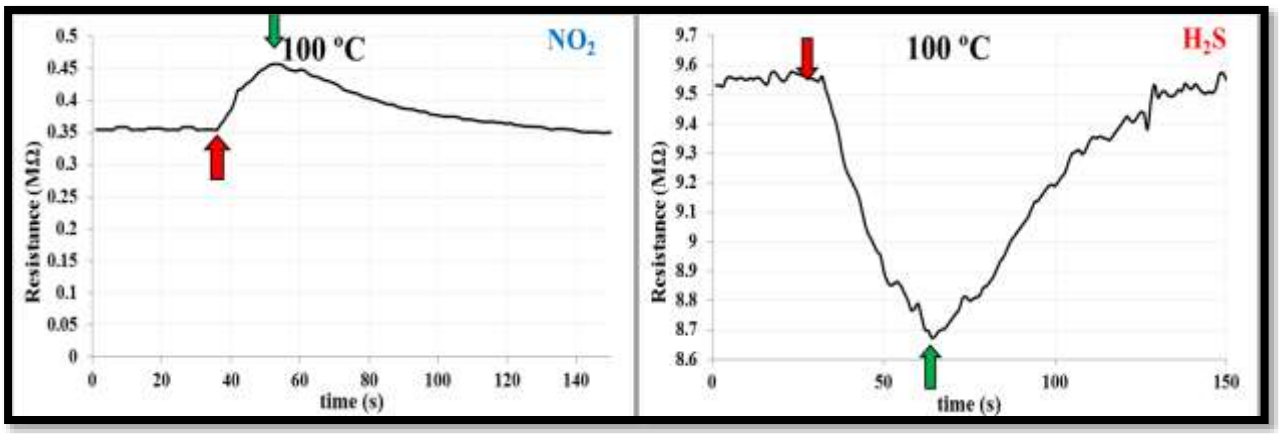

Academic Science Journal

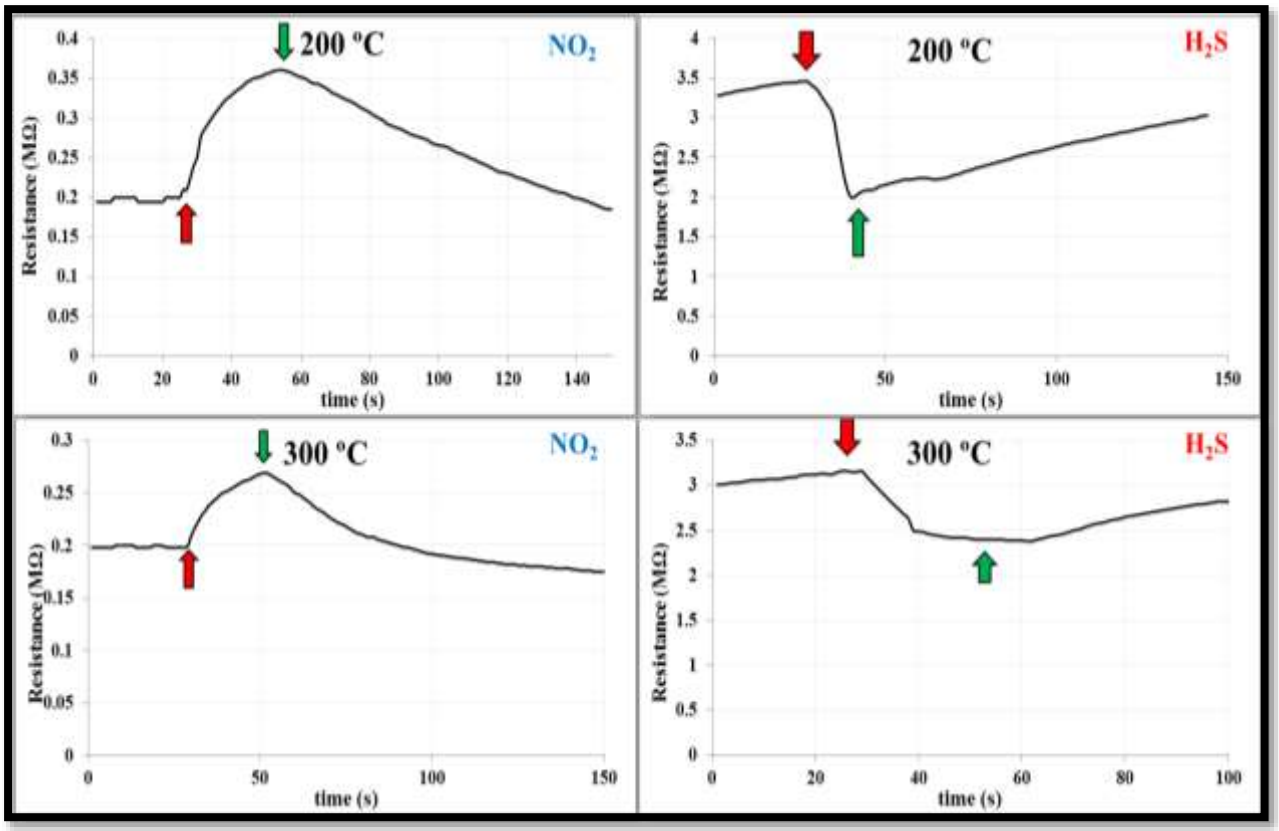

Figure 8: Resistance variation against 125 ppm NO_2 and 50 ppm H_2S for the pure CdO sensor prepared by Sol-gel technique.

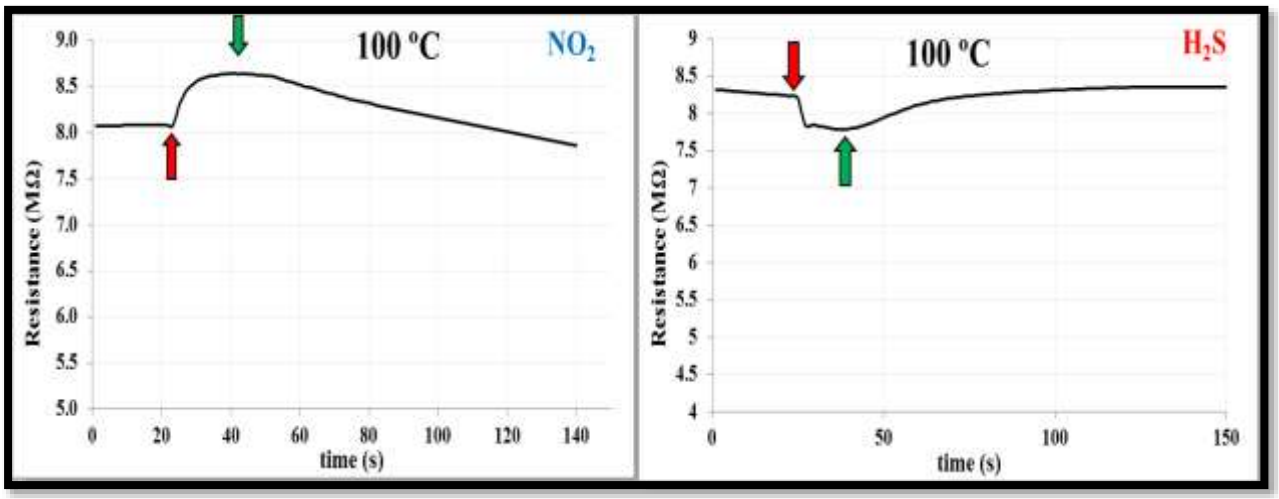

Academic Science Journal

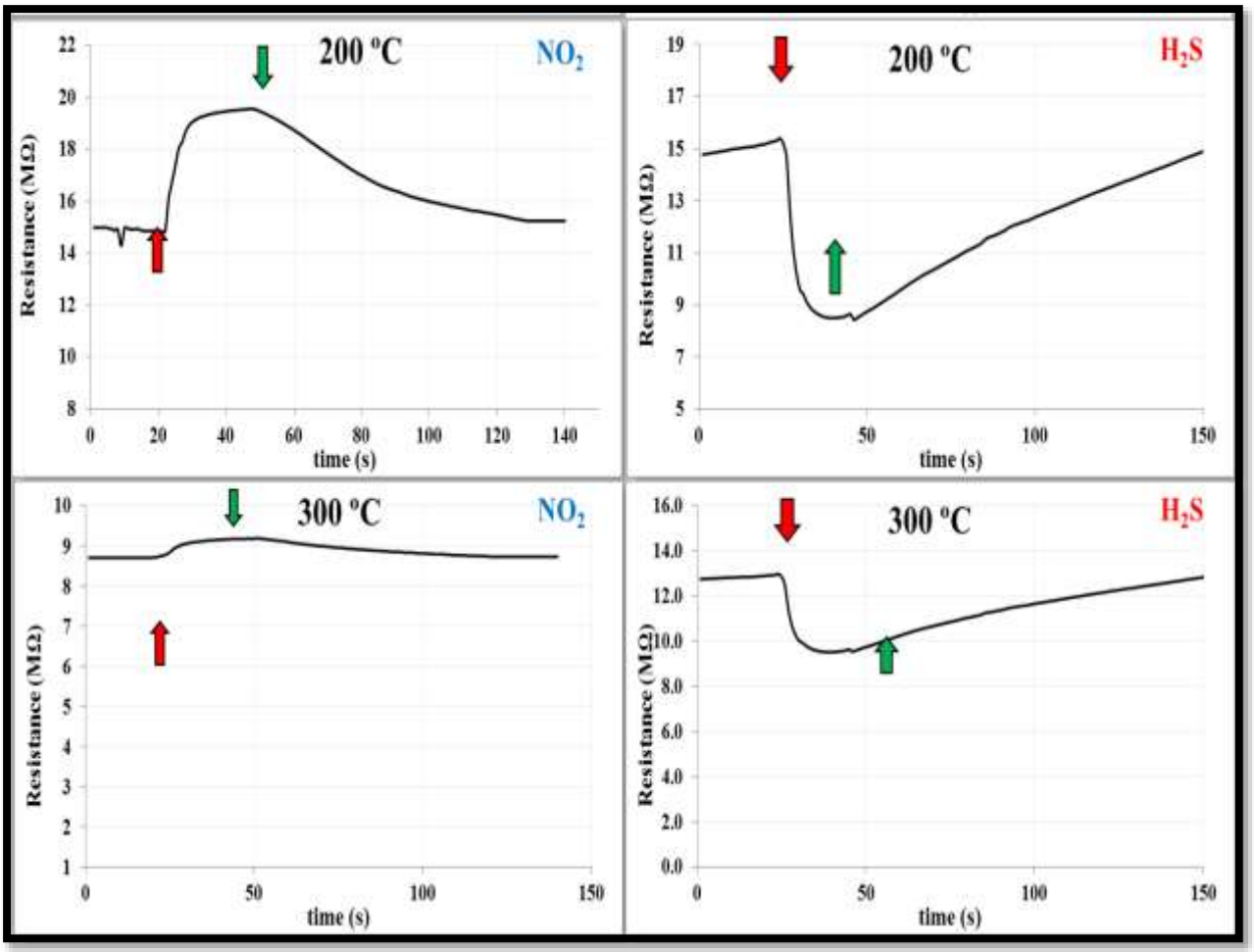

Figure 9: Resistance variation against 125 ppm NO_2 and 50 ppm H_2S for the CdO thin films dual-doped with 1%Cu and 1%Zn.

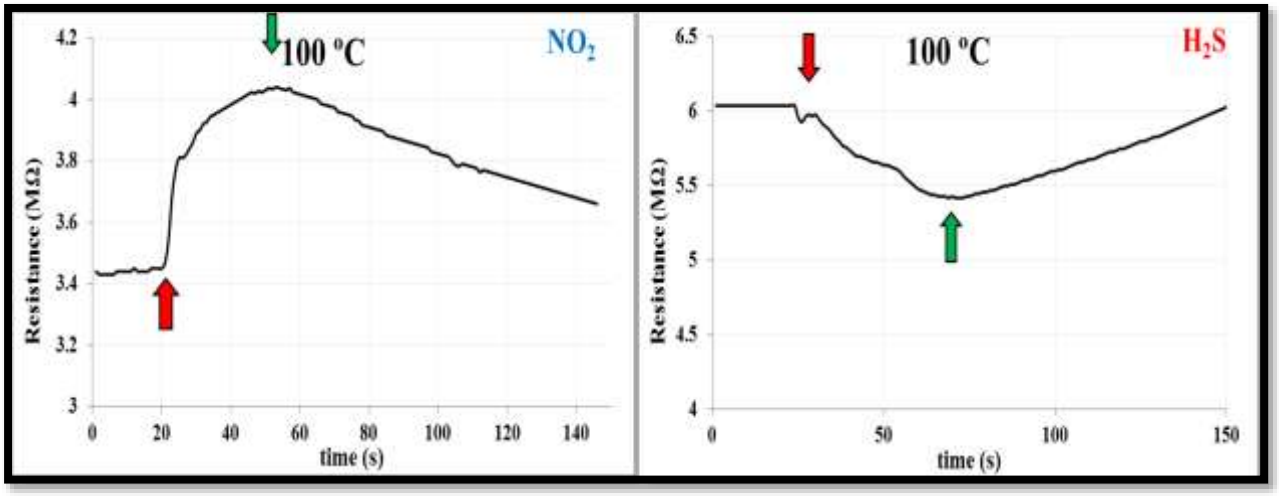

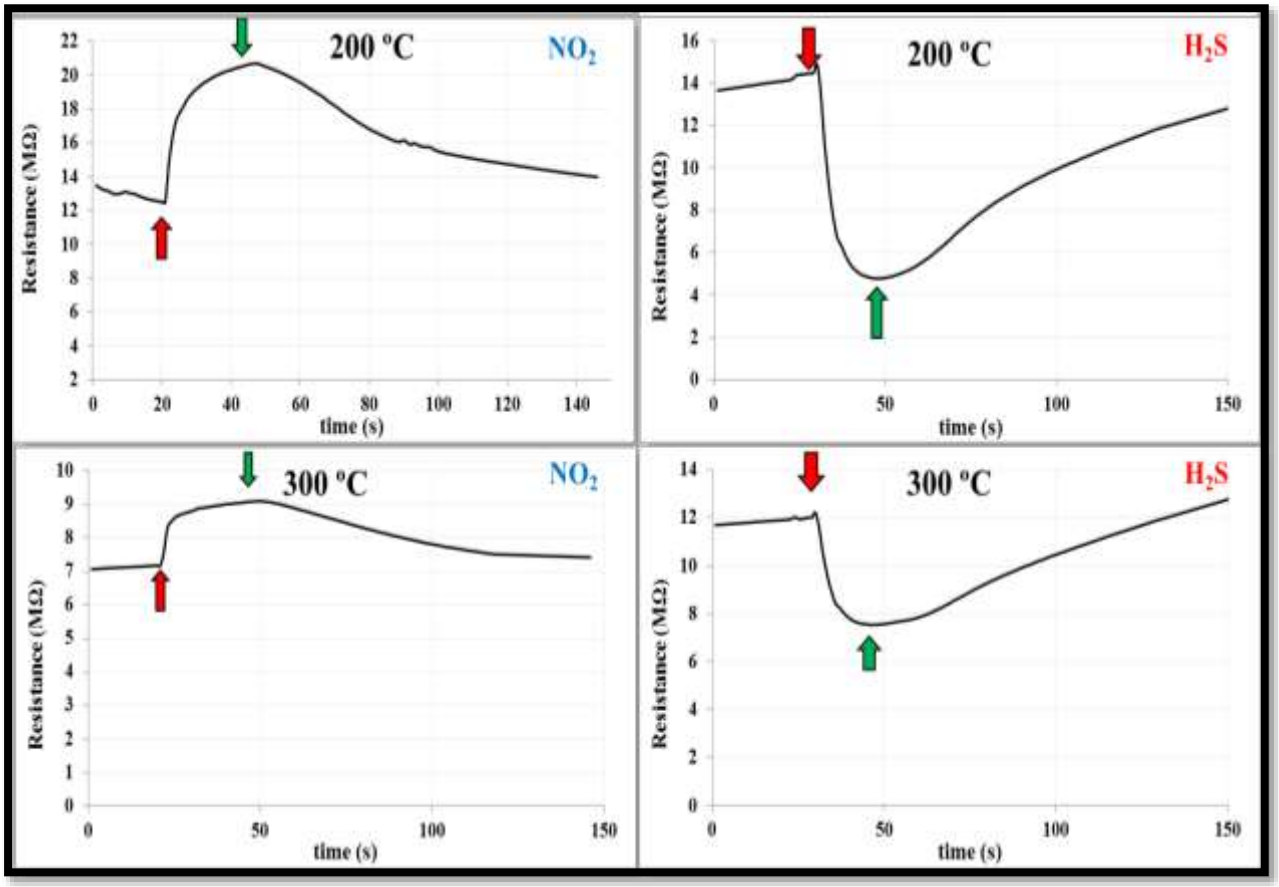

Figure 10: Resistance variation against 125 ppm NO_2 and 50 ppm H_2S for the CdO thin films dual-doped with 3%Cu and 3%Zn.

The method of computation described in reference [30] along with Equation (7) were used to determine the sensitivity of the sensor.

$$S = \left|\frac{R_g - R_a}{R_a}\right| \times 100\% \qquad (7)$$

where Ra and Rg, symbolize the film's resistance in the presence of air and gas, respectively, and S, the sensitivity [31]. Goal gases H_2S and NO_2 were utilized in the experiment at consistent concentrations. The gas sensitivity of spin-coated thin-film samples of pure CdO and (Zn:Cu) wt.% CdO co-doping is shown in Figure (11). Plotting the sensitivity against operating temperature is done with the presence of NO_2 and H_2S gases. The several kinds and quantities of oxygen that assimilation on the surface of the samples are responsible for the noticed changes

in sensitivity at various temperatures. The gas sensitivity mechanisms rely heavily on these oxygen species [32]. The pure CdO and (3% Zn:3% Cu) co-doped samples showed the highest sensitivity against the NO_2 and H_2S gases at 200°C, respectively. Consistent with other study findings, the deposition circumstances have a significant impact on the gas sensitivity of thin films. Also the increase in the mobility of carriers and the diffusion length improves the sensitivity of the gas because the possibility of electrons reaching the electrode increases without recombining with defects [33]. The relationship between the grains and the sample surfaces' roughness are two possible causes of this. Moreover, one of the most important factors influencing the samples' sensitivity is the existence of oxygen vacancies.

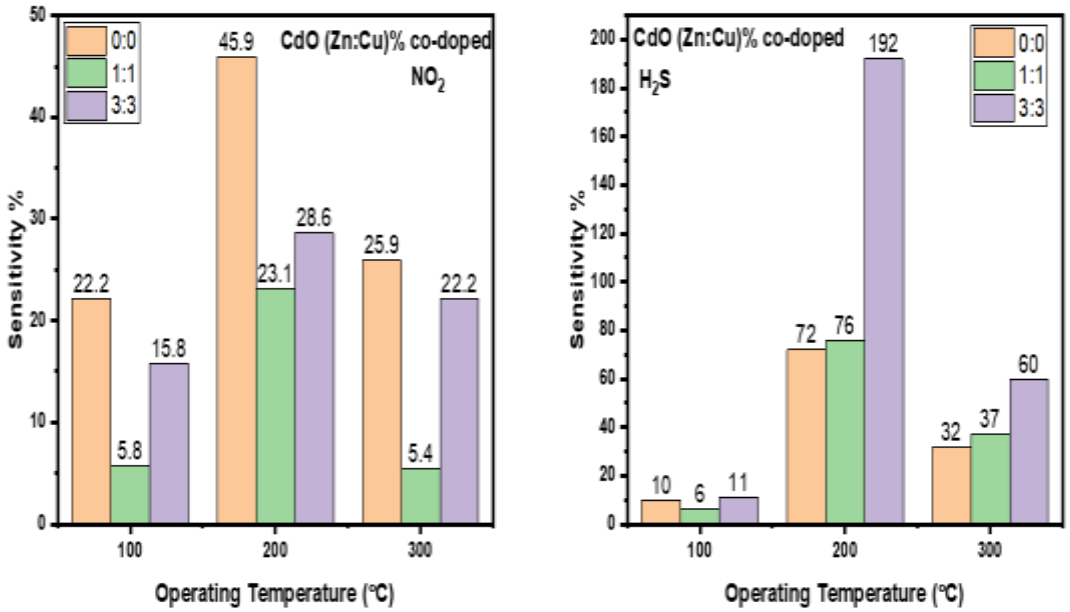

Figure 11: NO_2 and H_2S gases sensitivity versus operating temperature for pure CdO and (Zn:Cu) co-doping CdO thin films prepared by So-gel technique.

When an oxidizing or reducing gas is introduced, the response time of a gas sensor is the amount of time required for the conductance of the sensor to reach 90% of its highest or minimum value, respectively. Equation (8) expresses this. In a similar vein, as shown by Eq. (9) [34], the recovery time represents the amount of time needed for the sensor's resistance to recover to approximately 10% of the initial value following the cessation of the flow of gas.

Academic Science Journal

$$respons\ time = \left|t_{gas\ (on)} - t_{gas\ (off)}\right| \times 0.9 \quad (8)$$

$$recovery\ time = \left|t_{gas\ (off)} - t_{gas\ (recovery)}\right| \times 0.9 \quad (9)$$

The relation between the recovery time and response time of (Zn:Cu) wt.% co-doped CdO thin films and pure CdO at (100, 200, and 300) operating temperatures is shown in Figure (12). The graph shows that the NO_2 gas responds quickly (18 seconds) and recovers in 60 seconds, whereas the H_2S gas responds (27 seconds) and recovers in 45 seconds. This shows that when there is enough gas present for the intended reaction to happen, the NO_2 and H_2S gas sensors respond quickly. The desorption process is mainly responsible for the greater recovery time in comparison to the reaction time in gas detectors. When the goal gas is detected and a response is set off, the gas atoms are assimilation on the detector's surface, changing the electrical characteristics of the device. But after the gas is gone, it takes some time for the sensor to desorb or remove the gas atoms from their shallow and go back to their original form [35, 36].

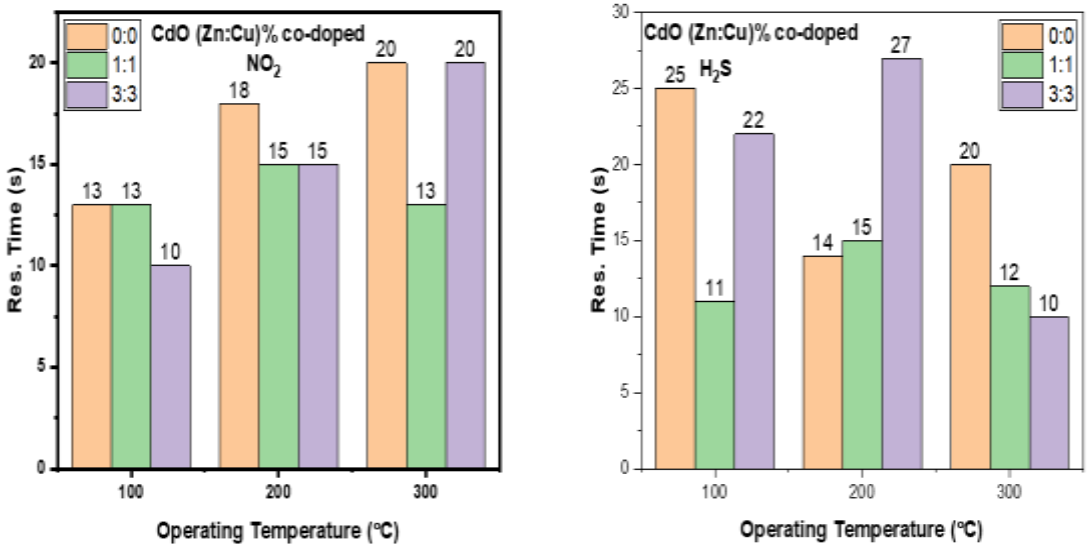

Academic Science Journal

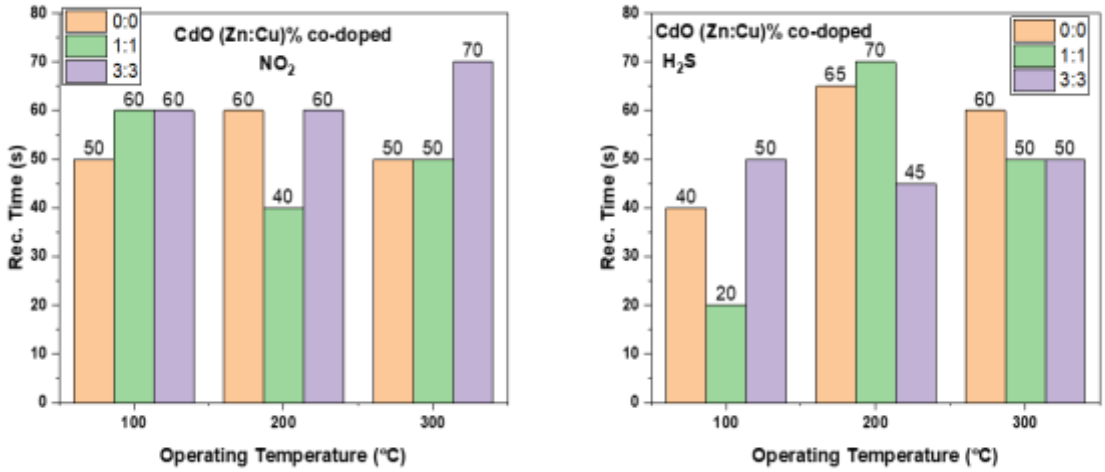

Figure 12: The relation of operating temperature, recovery time, and response time of NO_2 and H_2S gases for pure CdO and (Zn:Cu) co-doping CdO thin films prepared by So-gel technique.

Conclusion

The present research is the first report on the investigation of effect of (Zn:Cu) co-doping CdO on the gas sensitivity. This study investigated the structural, morphological, optical and electrical properties of (Zn:Cu)% co-doped CdO thin films. The thin films were successfully fabricated using the sol-gel spin coating technique on glass substrates. Gas-sensing measurements revealed that the pure CdO thin film exhibited the highest sensitivity to NO_2 gas while, the (3%Zn:3%Cu) co-doped CdO thin-film sample showed the highest sensitivity to H_2S gas. The results clearly demonstrate that the (Zn:Cu)% co-doping of CdO thin films enhances their selectivity toward hydrogen sulfide gas. This improved selectivity can be attributed to the changes in the structural, morphological and electrical properties induced by the co-doping process. The findings of this study highlight the potential of (Zn:Cu)% co-doped CdO thin films for gas sensing applications, particularly in the detection of NO_2 and H_2S gases. The ability to tailor structural, optical, and gas-sensing properties through co-doping makes these materials promising candidates for the development of advanced gas sensors.

Source of funding: This research received no funding.

Conflict of interest: The authors declare that there is no conflict of interest.

Ethical clearance: Ethical approval was not required for this review.

References

[1] A. Kumar, N. Sharma, A. P. Gutal, D. Kumar, P. Kumar, M. Paranjothy, M. Kumar, Growth and NO_2 gas sensing mechanisms of vertically aligned 2D SnS2 flakes by CVD: Experimental and DFT studies, Sensors and Actuators B: Chemical, 353, 131078(2022), DOI(https://doi.org/10.1016/j.snb.2021.131078)

[2] T. Seiyama, A. Kato, K. Fujiishi, M. Nagatani, A new detector for gaseous components using semiconductive thin films, Analytical Chemistry, 34(11), 1502-1503(1962)

[3] S. K. Pandey, K. H. Kim, K. T. Tang, A review of sensor-based methods for monitoring hydrogen sulfide, TrAC Trends in Analytical Chemistry, 32, 87-99(2012), DOI(https://doi.org/10.1016/j.trac.2011.08.008)

[4] E. Ashori, F. Nazari, F. Illas, Adsorption of H_2S on carbonaceous materials of different dimensionality, International Journal of Hydrogen Energy, 39(12), 6610-6619(2014), DOI(https://doi.org/10.1080/10962247.2018.1536004)

[5] N. Barsan, M. Schweizer-Berberich, W. Göpel, Fundamental and practical aspects in the design of nanoscaled SnO2 gas sensors: a status report, Fresenius' journal of analytical chemistry, 365, 287-304(1999), DOI(https://doi.org/10.1007/s002160051490)

[6] G. F. Fine, L. M. Cavanagh, A. Afonja, R. Binions, Metal oxide semi-conductor gas sensors in environmental monitoring, Sensors, 10(6), 5469-5502(2010), DOI(https://doi.org/10.3390/s100605469)

[7] J. Zhang, Z. Qin, D. Zeng, C. Xie, Metal-oxide-semiconductor based gas sensors: screening, preparation, and integration, Physical Chemistry Chemical Physics, 19(9), 6313-6329(2017), DOI(https://doi.org/10.1039/C6CP07799D)

[8] X. Liu, S. Cheng, H. Liu, S. Hu, D. Zhang, H. Ning, A survey on gas sensing technology, Sensors, 12(7), 9635-9665(2012), DOI(https://doi.org/10.3390/s120709635)

[9] S. P. Lee, Electrodes for semiconductor gas sensors, Sensors, 17(4), 683(2017), DOI(https://doi.org/10.3390/s17040683)

[10] C. R. Bobade, Cadmium oxide thin films synthesized at low temperature by spray CVD technique for H2S gas sensing applications, I J R B A T, Issue (VI), Vol. II, 118-125(2018)

[11] B. Şahin, Dual doping (Cu with rare-earth element Ce): An effective method to enhance the main physical properties of CdO films, Superlattices and Microstructures, 136, 106296(2019), DOI(https://doi.org/10.1016/j.spmi.2019.106296)

[12] B. R. Kumar, K. H. Prasad, K. Kasirajan, M. Karunakaran, V. Ganesh, Y. Bitla, I. S. Yahia, Enhancing the properties of CdO thin films by co-doping with Mn and Fe for photodetector applications, Sensors and Actuators A: Physical, 319, 112544(2021), DOI(https://doi.org/10.1016/j.sna.2021.112544)

[13] M. Ravikumar, R. Chandramohan, K. D. A. Kumar, S. Valanarasu, V. Ganesh, M. Shkir, A. Kathalingam, Effect of Nd doping on structural and opto-electronic properties of CdO thin films fabricated by a perfume atomizer spray method, Bulletin of Materials Science, 42, 1-10(2019), DOI(https://doi.org/10.1007/s12034-018-1688-x)

[14] M. Shkir, V. Ganesh, S. AlFaify, I. S. Yahia, H. Y. Zahran, Tailoring the linear and nonlinear optical properties of NiO thin films through Cr 3+ doping, Journal of Materials Science: Materials in Electronics, 29, 6446-6457(2018), DOI(https://doi.org/10.1007/s10854-018-8626-y)

[15] S. Valanarasu, V. Dhanasekaran, M. Karunakaran, T. A. Vijayan, R. Chandramohan, T. Mahalingam, Microstructural, optical and electrical properties of various time annealed spin coated MgO thin films, Journal of Materials Science: Materials in Electronics, 25, 3846-3853(2014), DOI(https://doi.org/10.1007/s10854-014-2098-5)

[16] K. S. Mohammed, J. M. Mansoor, J. Alzanganawee, S. Iftimie, , An investigation of annealing and (Zn+ Co) co-loading impact on certain physical features of nano-

structured (CdO) thin films coated by a sol-gel spin coating process, Journal of Ovonic Research, 17(5), (2021), DOI(https://doi.org/10.15251/JOR.2021.175.447)

[17] H. Kim, J. S. Horwitz, G. P. Kushto, S. B. Qadri, Z. H. Kafafi, D. B. Chrisey, Transparent conducting Zr-doped In2O3 thin films for organic light-emitting diodes, Applied Physics Letters, 78(8), 1050-1052(2001), DOI(https://doi.org/10.1063/1.1350595)

[18] M. K. Khalaf, B. A. ALhilli, A. I. Khudiar, A. Abd Alzahra, Influence of nanocrystalline size on optical band gap in CdSe thin films prepared by DC sputtering, Photonics and Nanostructures-Fundamentals and Applications, 18, 59-66(2016), DOI(https://doi.org/10.1016/j.photonics.2016.01.001)

[19] K. A. Aadim, A. H. Khidhir, Effect of Zinc (Zn)-Doped on the Structural, Optical and Electrical Properties of (Cdo) 1-Xznx Films Prepared by Pulsed Laser Deposition Technique, Iraqi Journal of Physics, 19(51), 64-71(2021), DOI(https://doi.org/10.30723/ijp.v19i51.676)

[20] M. Anitha, N. Anitha, K. Saravanakumar, I. Kulandaisamy, L. Amalraj, Effect of Zn doping on structural, morphological, optical and electrical properties of nebulized spray-deposited CdO thin films, Applied Physics A, 124, 1-13(2018), DOI(https://doi.org/10.1007/s00339-018-1993-7)

[21] T. Noorunnisha, M. Suganya, M. Karthika, C. Kayathiri, K. Usharani, S. Balamurugan, A. R. Balu, (Zn+ Co) co-doped CdO thin films with improved figure of merit values and ferromagnetic orderings with low squareness ratio well suited for optoelectronic devices and soft magnetic materials applications, Applied Physics A, 126, 1-9(2020), DOI(https://doi.org/10.1007/s00339-020-03954-z)

[22] A. Eskandari, F. Jamali-Sheini, Sonochemical synthesis of Cu-doped CdO nanostructures and investigation of their physical properties, Materials Science in Semiconductor Processing, 74, 210-217(2018), DOI(https://doi.org/10.1016/j.mssp.2017.08.028)

[23] A. H. K. Elttayef, H. M. Ajeel, A. I. Khudiar, Effect of annealing temperature and doping with Cu on physical properties of cadmium oxide thin films, Journal of Materials Research and Technology, 2(2), 182-187(2013), DOI(https://doi.org/10.1016/j.jmrt.2013.02.004)

[24] K. Usharani, A. R. Balu, Properties of spray deposited Zn, Mg incorporated CdO thin films, Journal of Materials Science: Materials in Electronics, 27, 2071-2078(2016), DOI(https://doi.org/10.1007/s10854-015-3993-0)

[25] G. Selvan, M. P. Abubacker, A. R. Balu, Structural, optical and electrical properties of Cl-doped ternary CdZnS thin films towards optoelectronic applications, Optik, 127(12), 4943-4947(2016), DOI(https://doi.org/10.1007/s10854-015-3993-0)

[26] S. Jin, Y. Yang, J. E. Medvedeva, J. R. Ireland, A. W. Metz, J. Ni, T. J. Marks, Dopant ion size and electronic structure effects on transparent conducting oxides Sc-doped CdO thin films grown by MOCVD, Journal of the American Chemical Society, 126(42), 13787-13793(2004), DOI(https://doi.org/10.1021/ja0467925)

[27] Bel-Hadj-Tahar, R., & Mohamed, A. B., Sol-gel processed indium-doped zinc oxide thin films and their electrical and optical properties, New Journal of Glass and Ceramics, 4(4), 55-65(2014), DOI(https://doi.org/10.4236/njgc.2014.44008)

[28] A. Staerz, U. Weimar, N. Barsan, Current state of knowledge on the metal oxide based gas sensing mechanism, Sensors and Actuators B: Chemical, 358, 131531(2022), DOI(https://doi.org/10.1016/j.snb.2022.131531)

[29] J. C. Hsieh, C. J. Liu, Y. H. Ju, Response characteristics of lead phthalocyanine gas sensor: effects of film thickness and crystal morphology, Thin Solid Films, 322(1-2), 98-103(1998), DOI(https://doi.org/10.1016/S0040-6090(97)00964-4)

[30] L. A. Patil, A. R. Bari, M. D. Shinde, V. V. Deo, D. P. Amalnerkar, Synthesis of ZnO nanocrystalline powder from ultrasonic atomization technique, characterization, and its application in gas sensing, IEEE Sensors journal, 11(4), 939-946(2010), DOI(https://doi.org/10.1109/JSEN.2010.2066265)

[31] L. Fan, X. Yang, H. Sun, A novel flexible sensor for double-parameter decoupling measurement of temperature and pressure with high sensitivity and wide range, Journal of Materials Chemistry C, 11(30), 10163-10177(2023), DOI(https://doi.org/10.1039/D3TC01636F)

[32] F. Challali, D. Mendil, T. Touam, T. Chauveau, V. Bockelée, A. G. Sanchez, M. P. Besland, Effect of RF sputtering power and vacuum annealing on the properties of AZO thin films prepared from ceramic target in confocal configuration, Materials Science in Semiconductor Processing, 118, 105217(2020), DOI(https://doi.org/10.1016/j.mssp.2020.105217)

[33] R. Tanuma, H. Haga, M. Sugiyama, Influence of carrier mobility on sensitivity of room-temperature-operation CO_2 sensor based on SnO_2 thin film, Japanese Journal of Applied Physics, 57(11), 115503(2018), DOI(https://doi.org/10.35848/1347-4065/ad358e)

[34] N. K. Abbas, I. M. Ibrahim, M. A. Saleh, Characteristics of MEH-PPV/Si and MEH-PPV/PS heterojunctions as NO_2 gas sensors, Silicon, 10, 1345-1350(2018), DOI(https://doi.org/10.1007/s12633-017-9610-5)

[35] S. Pagidi, K. S. Pasupuleti, M. Reddeppa, S. Ahn, Y. Kim, J. H. Kim, M. Y. Jeon, Resistive type NO_2 gas sensing in polymer-dispersed liquid crystals with functionalized-carbon nanotubes dopant at room temperature, Sensors and Actuators B: Chemical, 370, 132482(2022), DOI(https://doi.org/10.1016/j.snb.2022.132482)

[36] M. K. Khalaf, B. T. Chiad, A. F. Ahmed, F. A. Mutlak, Thin film technique for preparing nano-ZnO gas sensing (O_2, NO_2) using Plasma Deposition, Int. J. Appl. Innov. Eng. Manag, 2, 178-184(2013)